Archives of Hydro-Engineering and Environmental Mechanics
Vol. 50 (2003), No. 3, pp. 251–268

Finite Element Simulations of Floating Ice – Engineering Structure Interactions

Ryszard Staroszczyk

Institute of Hydro-Engineering of the Polish Academy of Sciences
ul. Waryńskiego 17, 71-310 Szczecin, Poland
Present address: School of Mathematics, University of East Anglia,
Norwich NR4 7TJ, United Kingdom. e-mail: r.staroszczyk@uea.ac.uk

(Received May 20, 2003; revised September 01, 2003)

Abstract

In this paper the problem of interaction between a coherent floating ice cover and a rigid engineering structure is considered. It is assumed that the ice cover, of horizontal dimensions considerably larger than the dimensions of the structure, is driven by wind and water current drag forces. During the interaction process of a quasi-static character, ice is assumed to behave as a creeping material, with a rheology described by the viscous fluid flow law. The ice cover is treated as a plate which sustains both bending due to the vertical reaction of the underlying water and the action of horizontal forces, which gives rise to the development of creep buckles in the plate and subsequently leads to the flexural failure of ice. An approximate solution to the problem is constructed by employing the finite element method. The results of numerical simulations illustrate the magnitudes of the forces exerted on the structure and their dependence on the wind direction and the structure geometry. In addition, the ice plate deflection in the vicinity of the structure is illustrated, and the values of the critical time at which the plate starts to fail by creep buckling are determined to show their dependence on the ice thickness, temperature, and type.

Key words: floating ice, plate, creep buckling, finite element method

Notations

C_a, C_w	–	dimensionless air and water drag coefficients,
D_{xx}, D_{yy}, D_{xy}	–	strain-rate tensor components,
g	–	gravitational acceleration,
H_1, H_2	–	parameters defining in-plane viscous behaviour of a plate,
h	–	plate thickness,
M_x, M_y	–	bending moments per unit width of a plate,

M_{xy} – twisting moment per unit width of a plate,
N_x, N_y – axial in-plane forces per unit width of a plate,
N_{xy} – shear in-plane force per unit width of a plate,
Q_x, Q_y – transverse shear forces per unit width of a plate,
q – distributed transverse load intensity,
R, R_1, R_2 – parameters defining flexural viscous behaviour of a plate,
T – ice temperature,
u_a, u_w – wind and water current velocities,
v_x, v_y – horizontal ice velocity components,
w – plate deflection,
x, y, z – rectangular Cartesian coordinates,
z_0 – plate neutral plane position,
ζ, ζ_a – bulk and axial viscosities of ice,
κ_x, κ_y – curvatures of a plate deflection surface,
κ_{xy} – twist of a plate deflection surface,
μ – shear viscosity of ice,
ϱ_a, ϱ_w – air and water densities,
$\sigma_{xx}, \sigma_{yy}, \sigma_{xy}$ – Cauchy stress tensor components,
τ_x, τ_y – distributed in-plane load intensity.

1. Introduction

As modern engineering activities advance into high-latitude regions, the issue of proper identification of loads exerted by floating ice on marine structures, such as drilling rigs, artificial islands, lighthouses, breakwaters or bridge piers, is of ever increasing importance. Therefore, in recent years, considerable research effort has been concentrated on the development of analytical and experimental methods helping to design and build reliable and cost-effective off-shore constructions. Obviously, a significant and indispensable, part of this process is the analysis of the mechanical behaviour of floating ice itself, since this yields design loads to which an engineering structure is subjected during its contact with the ice cover.

When a structure interacts with a coherent floating ice field driven by natural forces, such as wind and water drag, then three typical stages of the ice behaviour can usually be distinguished. During the first stage of loading, ice deforms mainly due to viscous creep, and behaves in a ductile, continuous manner, with the magnitudes of forces exerted on the structure increasing steadily in a regular fashion. With increasing ice deformation the next phase begins, in which cracks develop in the material, marking the onset of its failure, and ice undergoes a transition from ductile to brittle behaviour, which is also, a more or less, smooth process. This

second, relatively short-lasting transition period, is followed by the third stage of fully brittle fracture of ice, with the contact loads between the ice cover and the structure varying irregularly, as different parts of ice crush at different times. An important feature, from the point of view of an engineer, is the fact (Sanderson 1988) that the forces exerted by ice on the structure reach maximum magnitudes during the ductile-to-brittle transition phase. This feature allows us to simplify the designing process substantially, since the complex analysis requiring the use of methods of fracture mechanics can be avoided.

In this work we are concerned only with the ductile behaviour of floating ice, up to the instant at which it starts to fail by either brittle crushing or flexural failure mechanisms. A quasi-static problem is addressed, in which it is supposed that the ice cover is coherent enough to be regarded as a continuous sheet lying on the free surface of sea, river, or lake water, rather than as a collection of loosely connected floes that interact with each other. Such conditions occur when young, near-shore landfast ice is formed under relatively calm weather conditions, before the action of waves and wind breaks the ice, causing its rafting and ridging, and thus destroying its initial flat and uniform form. We analyse the processes which typically develop in a matter of hours rather than seconds, and hence we are not interested here in dynamic impact problems in which single, and relatively small-area floes, hit a structure. Accordingly, the floating ice cover is treated as a plate, whose in-plane dimensions are significantly larger than the characteristic dimensions of the structure with which it interacts. Ice is treated as a creeping material, with the constitutive behaviour described by a viscous fluid flow law. To account for the strong dependence of ice viscosity on temperature, which varies with the depth of ice, the plate is assumed to be non-homogeneous along the vertical. An engineering structure in contact with the ice is supposed to be rigid and interact with the ice plate along vertical walls.

The problem is solved by employing the classical theory of thin plates resting on a liquid foundation. The plate is bent by forces resulting from the reaction of the underlying water, and is also subjected to in-plane loads caused by the tangential tractions due to wind and water current drag forces. The combination of transverse and compressive in-plane forces gives rise to the development of creep buckles in the plate, which grow with time and ultimately lead to the flexural failure of ice when the tensile stresses in the plate reach some critical level. In (Staroszczyk and Hedzielski 2003) we investigated the problem of creep buckling of a floating ice plate having, in the horizontal plane, the shape of a truncated wedge of semi-infinite length. The problem was simplified by treating it as one-dimensional in space, that is, by considering the plate as a beam of variable width. In this work we treat the problem as fully two-dimensional, which allows us to analyse more complex plate geometries and loading scenarios. The solution has been constructed by using the finite element formulation, and the results obtained illustrate the magnitudes of the forces sustained by the structure

and their dependence on the direction of wind and the characteristic dimensions of the structure. Furthermore, the variation of the ice plate deflection near the structure is shown, and the influence of such factors as the thickness, temperature, and type of ice at the critical times at which the plate starts to fail are investigated.

2. Governing Equations

We consider the behaviour of a coherent ice cover floating on the free surface of water. The ice is driven by horizontal drag forces coming from the action of wind and water currents, and in some places it interacts with an engineering structure, exerting forces on the latter. As the ice cover deforms, not only in the horizontal direction but also transversely, it undergoes vertical loading resulting from the reaction of the underlying water. In this analysis, the floating ice cover is treated as a plate that rests on a liquid foundation, and is subjected to the combined action of the lateral as well as in-plane forces. The definitions of these forces, together with the adopted frame of rectangular coordinates, are shown in Fig. 1a. The plate is assumed to be of uniform thickness, denoted by h, and to be in perfect contact with the underlying water (Fig. 1b). The z-axis, directed downwards, is chosen in such a way that $z = 0$ at the top surface of the plate, and

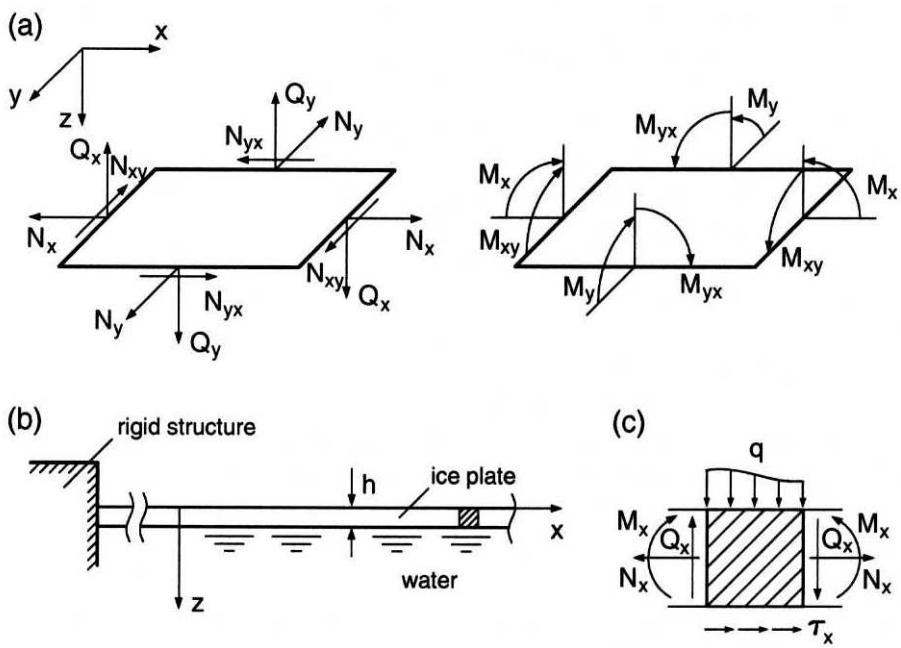

Fig. 1. (a) Adopted coordinate system and definitions of internal forces acting on a plate element, (b) and (c) vertical cross-sections of the plate along the x-axis

$z = h$ at the bottom surface. The plate transverse displacement along the z-axis is denoted by w. To account for a possible variation of the ice cover with depth and the influence of temperature, the plate is treated as non-homogeneous along the vertical, with the mechanical properties of ice supposed to be a function of depth. An engineering structure is modelled as a rigid body which interacts with the ice cover along vertical walls. The objective of the analysis is to calculate the forces exerted by the ice on an engineering structure, and to determine deformations and internal forces in the ice plate induced by the action of wind and water drag stresses.

In order to describe our problem, we employ the classical, linear theory of thin plates (Timoshenko and Woinowsky-Krieger 1959), based on the assumptions that the plate thickness is small compared with its characteristic lengths, the plate deflections are small, that is, not exceeding its thickness, and the plate cross-sections which are normal to the plate middle plane prior to deformation remain plane and normal to the middle surface in the deformed state.

In the horizontal plane Oxy, the only internal loads acting on a plate element are the axial forces N_x and N_y and the shear forces $N_{xy} = N_{yx}$, all measured per unit length. Apart from them, there are tangential forces distributed over the surfaces of the plate, caused by the wind and water drag. The two components of these tangential forces per unit area of the middle plane of the plate are denoted by τ_x and τ_y (see Fig. 1c). The equilibrium balances of the forces along the x and y axes, in the absence of inertia forces neglected here due to small horizontal velocities of ice, are expressed by the relations

$$\frac{\partial N_x}{\partial x} + \frac{\partial N_{xy}}{\partial y} + \tau_x = 0, \qquad \frac{\partial N_{xy}}{\partial x} + \frac{\partial N_y}{\partial y} + \tau_y = 0. \tag{1}$$

Along the z-axis, the plate is subjected to the vertical shear forces, Q_x and Q_y, and the transverse distributed load q. In the deformed state, the forces N_x, N_y and N_{xy}, all acting in directions tangential to the deflection surface $w(x, y)$, also have relevant vertical components. Hence, neglecting the weight of the ice, the projection of all forces on the z-axis gives

$$\begin{aligned} \frac{\partial Q_x}{\partial x} + \frac{\partial Q_y}{\partial y} + q + N_x \frac{\partial^2 w}{\partial x^2} + \frac{\partial N_x}{\partial x}\frac{\partial w}{\partial x} + N_y \frac{\partial^2 w}{\partial y^2} + \frac{\partial N_y}{\partial y}\frac{\partial w}{\partial y} \\ + 2N_{xy}\frac{\partial^2 w}{\partial x\,\partial y} + \frac{\partial N_{xy}}{\partial x}\frac{\partial w}{\partial y} + \frac{\partial N_{xy}}{\partial y}\frac{\partial w}{\partial x} = 0. \end{aligned} \tag{2}$$

Considering the equilibrium of moments acting on an infinitesimal plate element with respect to the y and x axes, we find that

$$\frac{\partial M_x}{\partial x} - \frac{\partial M_{xy}}{\partial y} - Q_x = 0, \qquad \frac{\partial M_y}{\partial y} - \frac{\partial M_{xy}}{\partial x} - Q_y = 0, \tag{3}$$

where M_x and M_y are the bending moments, and $M_{xy} = M_{yx}$ the twisting moments, all per unit length. The only transverse load that is exerted on the plate comes from the reaction of the underlying water. We assume that this reaction is elastic and treat the liquid base as the Winkler-Zimmerman-type foundation, in which case the response of the base is proportional to the plate deflection. Thus,

$$q = -\varrho_w g\, w, \tag{4}$$

where ϱ_w is the water density and g the acceleration due to gravity. We can now eliminate the vertical shearing forces Q_x and Q_y from (2) by determining them from (3). Using the relations (1) and (4) in (2) also, leads to the equation

$$\frac{\partial^2 M_x}{\partial x^2} - 2\frac{\partial^2 M_{xy}}{\partial x\,\partial y} + \frac{\partial^2 M_y}{\partial y^2} + N_x\frac{\partial^2 w}{\partial x^2} + 2N_{xy}\frac{\partial^2 w}{\partial x\,\partial y} + N_y\frac{\partial^2 w}{\partial y^2} - \varrho_w g\, w - \tau_x\frac{\partial w}{\partial x} - \tau_y\frac{\partial w}{\partial y} = 0, \tag{5}$$

involving the moments and in-plane loads, the plate deflection w and its derivatives, and the driving forces τ_x and τ_y. By expressing the internal forces in terms of the stresses in the plate, and then using constitutive relations to describe the properties of the material, we can transform equation (5) to one in which only the plate deformations appear. Hence, we define the in-plane axial and shear forces by

$$N_x = \int_0^h \sigma_{xx}\,\mathrm{d}z, \quad N_y = \int_0^h \sigma_{yy}\,\mathrm{d}z, \quad N_{xy} = \int_0^h \sigma_{xy}\,\mathrm{d}z, \tag{6}$$

and the bending and twisting moments by

$$M_x = \int_0^h \sigma_{xx} z\,\mathrm{d}z, \quad M_y = \int_0^h \sigma_{yy} z\,\mathrm{d}z, \quad M_{xy} = -\int_0^h \sigma_{xy} z\,\mathrm{d}z. \tag{7}$$

In the above relations, σ_{xx}, σ_{yy} and σ_{xy} are the stress tensor components. To proceed further, we need appropriate constitutive laws describing the material response of the ice.

The rheology of floating ice has been modelled in a number of ways, depending on the spatial and time scales involved, and also on the field of application. For instance, to describe the behaviour of a single ice floe on short-time scales the methods of viscoelasticity and fracture mechanics are commonly in use (Sanderson 1988), whereas the analysis of the behaviour of floating ice packs on geophysical scales requires quite different formalisms based on viscosity, viscoplasticity, and plasticity theories. An example of a constitutive theory for large-scale behaviour of sea ice is the widely used viscous-plastic model formulated by (Hibler 1979), in

which a viscous flow law is used for low strain-rates, and an associated plastic flow rule is applied for high strain-rates. This theory has subsequently been modified by using various shapes of the yield curve in the principal stress plane, ranging from an ellipse in the original formulation (Hibler 1979), through a teardrop shape (Rothrock 1975, Morland and Staroszczyk 1998), to straight lines for the cavitating fluid model (Flato and Hibler 1992). An alternative approach, in which the floating ice cover is treated as a non-linearly viscous fluid that satisfies the two-dimensional restrictions of the Reiner-Rivlin constitutive equation, has been pursued by Smith (1983) and Overland and Pease (1988). The predictions of these two classes of constitutive models (viscous-plastic against viscous) have been compared by Schulkes et al. (1988). Since in this work we are concerned with the off-shore applications in which the area of ice involved in the interaction with an engineering structure can be measured in square kilometres and more, we choose a constitutive theory which is relevant to large-scale modelling. Hence, we apply a constitutive relation of the Reiner-Rivlin type, previously used by Schulkes et al. (1998) and Morland and Staroszczyk (1998), expressed in the form

$$\sigma_{ij} = (\zeta - \mu) D_{kk} \delta_{ij} + 2\mu D_{ij} \quad (i, j, k = 1, 2), \tag{8}$$

where we adopt the summation convention for a repeated suffix. In (8), δ_{ij} is the Kronecker symbol, ζ and μ are the bulk and shear viscosities, respectively, and D_{ij} denotes the components of the two-dimensional strain-rate given by

$$D_{ij} = \frac{1}{2}\left(\frac{\partial v_i}{\partial x_j} + \frac{\partial v_j}{\partial x_i}\right) \quad (i, j = 1, 2), \tag{9}$$

where v_i constitute the components of the horizontal ice velocity vector $\mathbf{v}$, and the subscripts i and j stand for either x and y, with the equivalence $x_1 = x$ and $x_2 = y$. The definition (9), expressing the strain-rates in the neutral plane of the plate in terms of the in-plane velocity gradients alone, is consistent with the assumptions of the linear theory of small deflections of thin plates. However, which will be shown further in Section 4, see Figures 2 and 5, the deflections w at the plate failure can be of the order of the plate thickness h. Therefore, proper analytic treatment would require the application of the large-deflection plate theory, and hence the inclusion of the non-linear effects of the plate deflection slopes $\partial w/\partial x_j$ on the in-plane deformation of the plate (Timoshenko and Woinowsky-Krieger 1959). This would result (still assuming infinitesimal deformations in the neutral plane of the plate) in the appearance in the parentheses of (9) of an additional term $(\partial w/\partial x_i)(\partial \dot{w}/\partial x_j) + (\partial w/\partial x_j)(\partial \dot{w}/\partial x_i)$, where the superposed dot denotes the time derivative. To assess the importance of the latter non-linear term we note that in natural conditions the typical horizontal ice velocities v_i are of the order of 0.1 ms^{-1}, and they change over the scales of hundreds of metres. On the other hand, the vertical ice displacements w are of the order of the ice thickness

h, with the horizontal variations over distances of at least $10h$ (that is the buckle half-wavelengths), so $\partial w/\partial x_i$ is at most of the order 0.1, and this is attained over time scales of hours, say 10^4 s. Thus, the strain-rate terms involving the horizontal ice velocities are of the order of 10^{-3} s^{-1}, whereas those due to the vertical ice velocities are of the order of 10^{-5} s^{-1}, about 100 times smaller than the former. For this reason, the contribution of the non-linear term due to the plate deflection slope can be neglected in sea ice applications, hence the linear in the horizontal ice velocities relation (9) can be adopted for practical purposes.

In this study, we restrict attention to a linearly viscous fluid behaviour, in which both viscosities, ζ and μ, are independent of stress. However, since the viscous response of ice depends very strongly on temperature T, we incorporate this by assuming that

$$\frac{\zeta(T)}{\zeta(T_m)} = \frac{\mu(T)}{\mu(T_m)} = a^{-1}(\overline{T}), \tag{10}$$

where the scaling function $a(\overline{T})$, derived by Smith and Morland (1981), is given by

$$a(\overline{T}) = 0.68 \exp(12\,\overline{T}) + 0.32 \exp(3\,\overline{T}). \tag{11}$$

In the above relations, T_m denotes the ice melting temperatures, and $\overline{T}$ is a dimensionless temperature defined by $\overline{T} = (T - T_m)/[20°\text{C}]$.

Deformations in the ice cover can be expressed as the sum of the deformations in the neutral plane of the plate caused by the forces N_{ij}, and these can be regarded as a function of the horizontal coordinates x and y alone, and the deformations due to bending and twisting of the plate, which are functions of the depth z as well. Accordingly, the in-plane strain-rates are determined by using the horizontal velocity components $v_x(x, y)$ and $v_y(x, y)$ in (9), while the strain-rates due to bending and twisting are given in terms of the curvatures and twist of the deflection surface $w(x, y)$ as follows

$$D_{xx} = \dot{\kappa}_x z' = -\frac{\partial^2 \dot{w}}{\partial x^2} z', \quad D_{yy} = \dot{\kappa}_y z' = -\frac{\partial^2 \dot{w}}{\partial y^2} z', \quad D_{xy} = -\dot{\kappa}_{xy} z' = -\frac{\partial^2 \dot{w}}{\partial x\, \partial y} z'. \tag{12}$$

In these equations, κ_x and κ_y are the curvatures of the deflection surface along the x and y axes, respectively, κ_{xy} is the twist with respect to the x and y axes, and $z' = z - z_0$ is the distance from the neutral plane, with z_0 defining the position of the neutral plane in the undeformed state. With the strain-rates given by (9) and (12), and the stresses determined by the constitutive law (8), the in-plane axial and shear forces (6) become

$$N_x = (H_1 + H_2)\frac{\partial v_x}{\partial x} + (H_1 - H_2)\frac{\partial v_y}{\partial y},$$
$$N_y = (H_1 - H_2)\frac{\partial v_x}{\partial x} + (H_1 + H_2)\frac{\partial v_y}{\partial y}, \tag{13}$$
$$N_{xy} = H_2\left(\frac{\partial v_x}{\partial y} + \frac{\partial v_y}{\partial x}\right),$$

and the bending and twisting moments (7) are given by

$$M_x = -\left[(R_1 + R_2)\frac{\partial^2 \dot{w}}{\partial x^2} + (R_1 - R_2)\frac{\partial^2 \dot{w}}{\partial y^2}\right],$$
$$M_y = -\left[(R_1 - R_2)\frac{\partial^2 \dot{w}}{\partial x^2} + (R_1 + R_2)\frac{\partial^2 \dot{w}}{\partial y^2}\right], \tag{14}$$
$$M_{xy} = 2R_2\frac{\partial^2 \dot{w}}{\partial x\,\partial y}.$$

In the above expressions for the internal forces, the parameters defining the plate viscous properties are given by

$$H_1 = \int_0^h \zeta\,\mathrm{d}z,\quad H_2 = \int_0^h \mu\,\mathrm{d}z,\quad R_1 = \int_0^h \zeta z(z - z_0)\mathrm{d}z,\quad R_2 = \int_0^h \mu z(z - z_0)\mathrm{d}z. \tag{15}$$

By substituting now the definitions (14) for the internal moments into the equilibrium relation (5), we obtain the following differential equation

$$\frac{\partial^4 \dot{w}}{\partial x^4} + 2\frac{\partial^4 \dot{w}}{\partial x^2 \partial y^2} + \frac{\partial^4 \dot{w}}{\partial y^4} = \frac{1}{R}\left(N_x\frac{\partial^2 w}{\partial x^2} + 2N_{xy}\frac{\partial^2 w}{\partial x\,\partial y} + N_y\frac{\partial^2 w}{\partial y^2} - \varrho_w g\, w - \tau_x\frac{\partial w}{\partial x} - \tau_y\frac{\partial w}{\partial y}\right), \tag{16}$$

with

$$R = R_1 + R_2 = \int_0^h \zeta_a z(z - z_0)\mathrm{d}z, \tag{17}$$

where $\zeta_a = \mu + \zeta$ is called the axial viscosity. Equation (16) describes the time and space variation of plate displacement w in terms of the in-plane forces N_{ij} and the driving forces τ_i $(i, j = 1, 2)$. The forces N_{ij}, the functions of the plate horizontal velocities v_x and v_y, see (13), can be determined independently of (16) by solving the equations of the in-plane equilibrium (1). Typical boundary conditions, with which the three equations (16) and (1) are solved in sea ice applications, are those of a simply-supported plate edge in the contact region with the structure,

with zero horizontal velocities in the direction normal to the ice-structure interface (so-called free-slip conditions). These conditions are expressed by

$$w = 0, \quad M_n = 0, \quad \mathbf{v} \cdot \mathbf{n} = \mathbf{0}, \tag{18}$$

where n is the direction normal to the edge of the plate, defined by the unit vector $\mathbf{n}$, and M_n is the bending moment acting on the plate section normal to $\mathbf{n}$.

3. Finite Element Formulation

The system of three differential equations for the plate deflection w and the horizontal velocities v_x and v_y, given by (16) and (1) with (13), is solved approximately by applying the finite element method. The weighted residual, or Galerkin, version of the method is employed, in which the problem equations are satisfied in an integral mean sense. The plate is discretised in the horizontal plane Oxy by using a mesh of triangular elements, with the unknown variables defined at the corner nodes. In addition to the plate displacement and two horizontal velocity components, at each node also the plate slopes $\partial w/\partial x$ and $\partial w/\partial y$ are treated as separate unknown variables. Such an approach is typical of the plate theory and is applied in order to ensure the continuity of the plate slopes between elements (Zienkiewicz and Taylor 1991). Thus, at each node we have five discrete parameters to be calculated, three related to the plate bending, and two related to the in-plane deformation, hence altogether there are 15 degrees of freedom at each element. The continuous functions w, v_x and v_y are approximated by the following representations:

$$\begin{aligned} w(x,y,t) &= \Phi_j^w(x,y) w_j(t), \quad (j = 1, \ldots, 9), \\ v_i(x,y,t) &= \Phi_j^v(x,y) v_{ij}(t), \quad (i = 1, 2;\ j = 1, 2, 3), \end{aligned} \tag{19}$$

where t denotes time and w_j and v_{ij} are the unknown nodal parameters, displacements and velocities respectively, with the former including both the plate deflections and the plate slopes. Φ_j^w and Φ_j^v are shape (interpolation) functions, which are different for the displacements and the velocity fields. While the velocity field is interpolated by simple linear shape functions, for the plate deflection approximation we use the shape functions which are fourth-order polynomials in both x and y, in the formulation due to Specht (Zienkiewicz and Taylor 1991).

Following the typical finite element procedure, the problem equations (16) and (1) are multiplied by a set of continuous and sufficiently smooth weighting functions, which in the Galerkin method are identical with the element shape functions, here Φ_j^w and Φ_j^v, and the resulting relations are then integrated over the plate domain. In the process, in order to reduce the order of integration, we use the Green theorem (once for each equation involving the velocities and twice for each equation involving the plate deflection). With respect to the plate

displacement equations, it turns out that it is more straightforward to start first with the relation (5) and only then to apply the definitions (14) for the moments, rather than to proceed with the relation (16), although obviously the resulting final equations are identical. Using subsequently the approximations (1) and performing the prescribed integration, we reduce the problem on hand to the solution of a set of first-order differential equations given in a matrix form by

$$\mathbf{C}\dot{\mathbf{w}} + \mathbf{K}\mathbf{w} = \mathbf{f}, \tag{20}$$

where the vector $\mathbf{w}$ includes the values of the plate deflections w_l, the plate slopes $(\partial w/\partial x)_l$ and $(\partial w/\partial y)_l$, and the velocities v_{xl} and v_{yl} at all nodal points l of the discrete system. We note that in our problem the matrix $\mathbf{K}$ depends on the horizontal velocities, so $\mathbf{K} = \mathbf{K}(\mathbf{w})$. The matrices $\mathbf{C}$, $\mathbf{K}$, and the forcing vector $\mathbf{f}$ are aggregated from the respective single element matrices and vectors in a way characteristic of the finite element method. The element matrices, each 15×15 in size, are, in turn, composed of 9 submatrices each of dimensions 5×5. The non-zero entries in these component submatrices are given for the matrix $\mathbf{C}$ by

$$\begin{aligned} c_{rs}^{mn} = \int_A \Bigg[& (R_1 + R_2)\left(\frac{\partial^2 \Phi_i^w}{\partial x^2}\frac{\partial^2 \Phi_j^w}{\partial x^2} + \frac{\partial^2 \Phi_i^w}{\partial y^2}\frac{\partial^2 \Phi_j^w}{\partial y^2}\right) \\ & + 4R_2 \frac{\partial^2 \Phi_i^w}{\partial x\,\partial y}\frac{\partial^2 \Phi_j^w}{\partial x\,\partial y} + (R_1 - R_2)\left(\frac{\partial^2 \Phi_i^w}{\partial x^2}\frac{\partial^2 \Phi_j^w}{\partial y^2} + \frac{\partial^2 \Phi_i^w}{\partial y^2}\frac{\partial^2 \Phi_j^w}{\partial x^2}\right)\Bigg] \mathrm{d}A, \end{aligned} \tag{21}$$

and for the matrix $\mathbf{K}$ by

$$\begin{aligned} k_{rs}^{mn} &= \int_A \Phi_i^w \left(\varrho_w g \Phi_j^w + \tau_x \frac{\partial \Phi_j^w}{\partial x} + \tau_y \frac{\partial \Phi_j^w}{\partial y} - N_x \frac{\partial^2 \Phi_j^w}{\partial x^2} \right. \\ &\quad \left. -2N_{xy}\frac{\partial^2 \Phi_j^w}{\partial x\,\partial y} - N_y \frac{\partial^2 \Phi_j^w}{\partial y^2} \right) \mathrm{d}A, \\ k_{rs}^{44} &= \int_A \left[(H_1 + H_2)\frac{\partial \Phi_r^v}{\partial x}\frac{\partial \Phi_s^v}{\partial x} + H_2 \frac{\partial \Phi_r^v}{\partial y}\frac{\partial \Phi_s^v}{\partial y} \right] \mathrm{d}A, \\ k_{rs}^{45} &= \int_A \left[(H_1 - H_2)\frac{\partial \Phi_r^v}{\partial x}\frac{\partial \Phi_s^v}{\partial y} + H_2 \frac{\partial \Phi_r^v}{\partial y}\frac{\partial \Phi_s^v}{\partial x} \right] \mathrm{d}A, \\ k_{rs}^{54} &= \int_A \left[H_2 \frac{\partial \Phi_r^v}{\partial x}\frac{\partial \Phi_s^v}{\partial y} + (H_1 - H_2)\frac{\partial \Phi_r^v}{\partial y}\frac{\partial \Phi_s^v}{\partial x} \right] \mathrm{d}A, \\ k_{rs}^{55} &= \int_A \left[H_2 \frac{\partial \Phi_r^v}{\partial x}\frac{\partial \Phi_s^v}{\partial x} + (H_1 + H_2)\frac{\partial \Phi_r^v}{\partial y}\frac{\partial \Phi_s^v}{\partial y} \right] \mathrm{d}A. \end{aligned} \tag{22}$$

The indices in (21) and (22) are

$$r, s, m, n = 1, 2, 3, \quad i = 3(r-1) + m, \quad j = 3(s-1) + n, \tag{23}$$

and A denotes the plane domain of integration. The components of the forcing vector $\mathbf{f}$ are defined by

$$
\begin{aligned}
f_r^m &= \oint_\Gamma \Phi_i^w Q \mathrm{d}\Gamma, \\
f_r^4 &= \int_A \Phi_r^v \tau_x \mathrm{d}A + \oint_\Gamma \Phi_r^v T_x \mathrm{d}\Gamma, \\
f_r^5 &= \int_A \Phi_r^v \tau_y \mathrm{d}A + \oint_\Gamma \Phi_r^v T_y \mathrm{d}\Gamma,
\end{aligned}
\tag{24}
$$

where Γ denotes the boundary of the domain A. In the first equation, Q is the vertical shear force acting on the boundary Γ, and T_x and T_y are, respectively, the x and y components of the in-plane traction vector $\mathbf{T}$ acting on Γ, and are expressed by

$$
T_x = N_x n_x + N_{xy} n_y, \quad T_y = N_{xy} n_x + N_y n_y, \tag{25}
$$

with n_x and n_y denoting the components of the outward unit vector $\mathbf{n}$ normal to the boundary Γ.

The time-integration of the system of equations (20) is performed by using the so-called θ-method (the explicit Euler, Crank-Nicholson, and implicit Euler methods are all special cases of the θ-method, with the value of the θ parameter equal, respectively, to 0, 0.5, and 1). Application of the θ-method to (20) results in the relation that connects the solution vectors $\mathbf{w}_n$ and $\mathbf{w}_{n+1}$ at two consecutive time levels, t_n and t_{n+1}:

$$
(\mathbf{C} + \theta \Delta t \mathbf{K}) \mathbf{w}_{n+1} = [\mathbf{C} - (1-\theta)\Delta t \mathbf{K}] \mathbf{w}_n + \Delta t \tilde{\mathbf{f}}, \tag{26}
$$

where $\Delta t = t_{n+1} - t_n$ is the time-step length. The vector $\tilde{\mathbf{f}}$ is the time-averaged forcing vector which, assuming a linear variation of $\mathbf{f}$ from t_n to t_{n+1}, is defined by

$$
\tilde{\mathbf{f}} = (1-\theta)\mathbf{f}_n + \theta \mathbf{f}_{n+1}. \tag{27}
$$

In our numerical calculations, the value of $\theta = 0.6$ has been adopted, which guarantees that the time-discretisation error is nearly of the second-order (the value of $\theta = 0.5$ leads to the error of the order $(\Delta t)^2$, but in that case the scheme is not unconditionally stable).

4. Numerical Examples

In numerical calculations simulating the interaction of a floating ice cover with a rigid engineering structure we have assumed that the wind and water drag forces which drive the ice pack are related to the wind and water current velocities by means of the quadratic relations given by

$$\tau_a = C_a \varrho_a (u_a - v)^2, \qquad \tau_w = C_w \varrho_w (u_w - v)^2, \tag{28}$$

where τ_a and τ_w are the magnitudes of the tangential tractions per unit area due to the wind and water action, respectively, ϱ_a and ϱ_w are the air and water densities, u_a and u_w the velocities of wind and water current, and v is the horizontal velocity of ice in the direction of the respective driving force. The parameters τ_x and τ_y appearing in the equilibrium equations in Section 2 are equal to the sums of the projections of τ_a and τ_w on the respective coordinate axes. The parameters C_a and C_w in (28) are the dimensionless drag coefficients, for which, after Sanderson (1988), we have adopted the values $C_a = 2 \times 10^{-3}$ and $C_w = 4 \times 10^{-3}$. The air and water densities are $\varrho_a = 1.3$ kgm^{-3} and $\varrho_w = 1.02 \times 10^3$ kgm^{-3}, and $g = 9.81$ ms^{-2}. The results of simulations presented below have been obtained for the ice viscosities $\zeta = \mu = 1.0 \times 10^9$ kgm^{-1}s^{-1}. The temperature on the top surface of the ice, if not stated otherwise, is assumed to be -2°C, and that on the bottom surface to be 0°C. The critical tensile stress in ice, σ_{cr}, at which the plate is regarded to start to fail due to the development and subsequent opening of tensile cracks, has been assumed to be equal to 0.2 MPa. This value corresponds, approximately, to the presence in ice of vertically aligned cracks of a depth equal to $h/10$ (Sanderson 1988).

In order to verify the performance of the finite element model formulated in Section 3, we start with the numerical solution of a one-dimensional problem, for which a closed-form analytical solution is available (Staroszczyk and Hedzielski 2003). Accordingly, we consider the problem of creep buckling of a plate of a uniform width, with the plate lateral sides parallel to the x-axis. One end of the plate is in contact with a rigid wall situated at $x = 0$, with the simply-supported boundary conditions there, and the other end of the plate is loaded by a compressive axial force $N_x < 0$; no other driving loads are exerted on the plate, that is $\tau_x = \tau_y = 0$, and $N_y = N_{xy} = 0$ are assumed. Creep buckling requires initial perturbations of the plate deflections, otherwise (when $w(x, 0) = 0$) only elastic buckling is possible under the action of horizontal loading. Following Staroszczyk and Hedzielski (2003), the initial small displacements of the plate are adopted as a sum of twenty harmonic in x components, given by

$$w_0(x) = \sum_{i=1}^{20} \pm w_0^{(i)} \sin(i\pi x / L), \tag{29}$$

where the signs ($\pm$) are chosen at random, and all the component amplitudes $w_0^{(i)}$ are equal and such that the maximum initial deflection $w_0 = 0.001$ m. L, defining the longest half-wavelength of the initial perturbation, is chosen to be three times the length L_0, the latter denoting the length of the fastest growing creep buckle. L_0 is a function of the compressive load and the density of the underlying

liquid base (Sanderson 1988, Staroszczyk and Hedzielski 2003). Solution of the one-dimensional form of equation (16), with the initial condition (29), yields the relation describing the evolution of the plate displacement

$$w(x,t) = \sum_{i=1}^{20} \pm w_0^{(i)} \exp(t/\tau_i) \sin(\pi x / L_i), \quad L_i = L/i, \tag{30}$$

where the time constants τ_i are given by

$$\frac{1}{\tau_i} = \frac{1}{R}\left[-N_x \left(\frac{L_i}{\pi}\right)^2 - \varrho g \left(\frac{L_i}{\pi}\right)^4\right]. \tag{31}$$

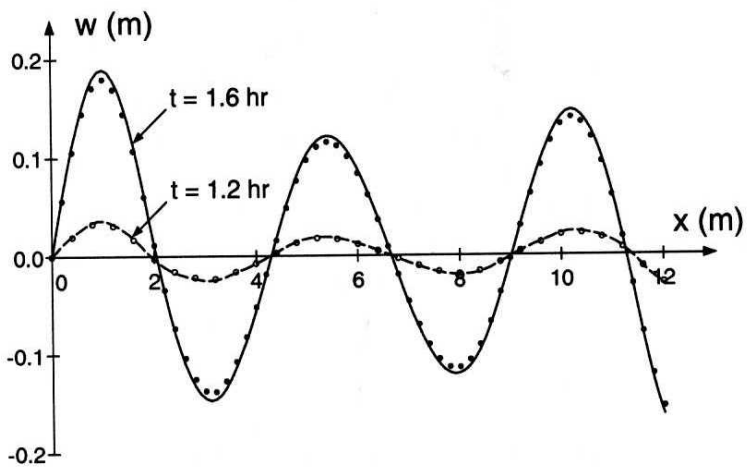

Fig. 2. Plate deflections w at two different times t (in hours) for a uniform-width plate of the ice thickness $h = 0.2$ m under the horizontal loading $N_x = -10^4$ Nm^{-1}. Compared are the finite element (circles) and analytical (lines) results

The results shown in Fig. 2 have been obtained for the ice plate thickness $h = 0.2$ m, subjected to the axial compressive force of the magnitude 1.0×10^4 Nm^{-1}. The plots illustrate the plate deflections $w(x)$ at later stages of the creep buckling process, close to the onset of flexural failure. The dashed and solid lines represent the analytical results for $t = 1.2$ hr and $t = 1.6$ hr, respectively (actually, the plate fails at $t = 1.69$ hr). The corresponding finite element results are shown, for the same times, by open and solid circles, respectively. It is seen in the figure that the maximum deflections before the critical time at which the plate breaks up can be as large as the plate thickness, and the plate deformations, just before the failure, consist, essentially, of buckles of the length close to L_0, here equal to 2.2 m. The comparison of the deflections obtained by the two methods indicates quite a good accuracy of the discrete method, with the results differing from each other by

no more than about 3%. Bearing in mind that in the example considered the shortest buckles have half-wavelengths smaller than the horizontal mesh spacing, this can be regarded as a very satisfactory performance of the numerical scheme constructed.

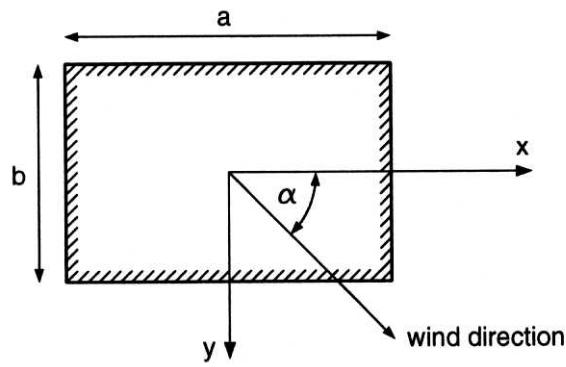

Fig. 3. A rectangular rigid structure of horizontal dimensions $a \times b$ interacting with ice driven by wind blowing at the angle α to the x-axis

Having verified the accuracy of the discrete model in the simple one-dimensional configuration, we proceed to a two-dimensional problem sketched in Fig. 3, in which we simulate the behaviour of the floating ice cover interacting with a rectangular in plane rigid structure of the horizontal dimensions defined by a and b. The ice cover is driven towards the structure by air drag forces caused by a wind blowing in the direction defined by the angle α shown in the figure. The simulations have been carried out for a structure situated at the centre of rectangular in a shape ice field 1 km $\times$ 1 km and ice thickness $h = 0.5$ m. At the ice-structure interface, the plate was simply-supported and free-slip boundary conditions (18) were adopted. The wind has been assumed to have a speed of $u_a = 30$ ms^{-1}, and its direction has been varied within the range $0 < \alpha < 90°$ to investigate how this affects the total loading exerted by ice on the structure. Three particular cases of the structures of different shapes have been considered, in which the width of the structure b is kept constant and equal to 10 m, and the length a is varied and equal to 20, 30 and 40 m, respectively. The results of numerical calculations, conducted with the mesh consisting of 4000 finite elements and 10400 degrees of freedom, are presented in Figure 4. The plots illustrate the dependence on the angle α of the total horizontal force F which the ice cover exerts on the structure; also shown are the components of the total force along the x and y axes, F_x and F_y respectively. The results obtained for the shortest rectangle 20 m $\times$ 10 m are represented by solid lines, those for the rectangle 30 m $\times$ 10 m are given in dashed lines, and those for the longest rectangle 40 m $\times$ 10 m are indicated by dashed-dotted lines. We see in the figure that, for the ice thickness and viscosities considered, the geometry of the rectangle has a relatively small effect on the total

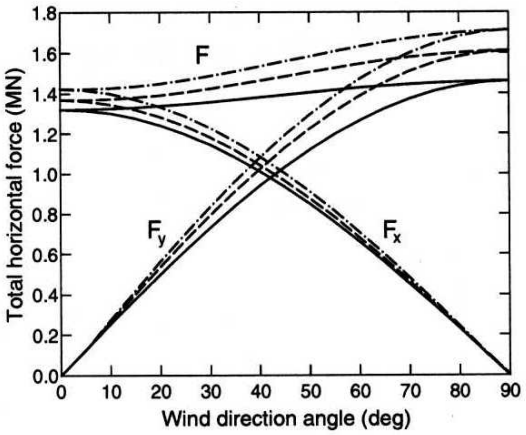

Fig. 4. Total horizontal forces F, together with their components F_x and F_y, exerted on the structure by the ice cover as a function of the wind direction angle α. Shown are the results for three rectangles of the same width $b = 10$ m and the lengths 20 m (solid lines), 30 m (dashed lines) and 40 m (dashed-dotted lines)

force F sustained by the structure. For wind blowing in a direction perpendicular to the longer side of the structure, $\alpha = 90°$, the magnitudes of the extremal forces F differ by 17.1%, and for the wind direction parallel to the longer side, $\alpha = 0°$, the respective relative difference is equal to 7.6%. We also note the relatively small influence of the direction of wind on the total force magnitude F. For the longest structure, for which $a/b = 4$, the maximum and minimum forces, for $\alpha = 90°$ and $\alpha = 0°$ respectively, differ by 20.1%, while for the shortest structure, for which $a/b = 2$, the corresponding relative difference is 10.5%. Also for different plate thicknesses, results of a similar character, that is showing a relatively small effect of the wind angle on the total force acting on a structure, have been obtained from the simulations. This suggests that also the influence of other factors influencing the ice rigidity, such as the ice temperature and type of anisotropy of ice, have little effect on the horizontal forces transmitted from the ice cover onto the structure.

The factors just indicated, that is those affecting the strength of ice, have, however, a significant influence on the behaviour of the ice cover in bending, and hence on the creep buckling of the ice plate. And this, in turn, under given loading conditions, determines the value of the critical time, prior to which ice behaves in a continuous manner, and after which the ice cover begins to break up, giving rise to a sequence of ice-structure interaction events irregular in time. For the particular case of the structure dimensions $a = 20$ m and $b = 10$ m, and for the wind blowing along the negative direction of the $x-$axis (that is for $\alpha = 180°$), the plate deflections along the positive x-axis occurring at the critical time at which the plate failure starts are shown in Fig. 5. The x-axis in this figure, compared to

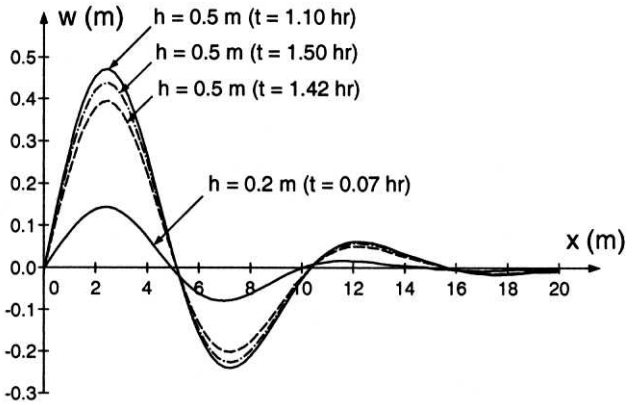

Fig. 5. Plate deflections w along the x-axis at critical times t (given in hours) for a wind direction angle $\alpha = 180°$. Shown are the results for a plate thickness $h = 0.2$ m and $h = 0.5$ m (solid lines); for the thicker plate also the deflections and corresponding critical times for colder (dashed line) and stronger (dashed-dotted line) ice are presented

Fig. 3, is shifted by $a/2$ so that $x = 0$ is the position of the ice-structure interface. The solid lines in the figure illustrate the deflections for two different ice plate thicknesses, $h = 0.2$ m and $h = 0.5$ m. We immediately note that the critical times for these two plates differ quite considerably: $t = 0.07$ hr (about 250 s) for the thinner ice and $t = 1.10$ hr for the thicker. The dashed line represents, for $h = 0.5$ m, the plate deflection in the case of the top surface of the ice cover having a temperature of $-4°$ C (recall that we have assumed everywhere an ice-free surface temperature equal to $-2°$ C). Finally, the dashed-dotted line displays, again for $h = 0.5$ m, the plate deflection for ice with both viscosities, ζ and μ, increased by 30%; such a difference in viscosities occurs between isotropic ice and transversely isotropic, so-called columnar, ice. We see that both temperature and the type of ice anisotropy have quite pronounced effects on the strength of ice, significantly increasing the values of the critical time (by about 30% in our example). On the other hand, the maximum plate deflections do not change considerably with the change of temperature and type of ice.

5. Conclusions

In the paper, the problem of the behaviour of a floating ice cover interacting with a rigid structure has been presented. The ice cover is treated as a plate made of a creeping material, resting on an elastic liquid base, and subjected to both transverse bending forces and in-plane loading due to natural forces driving the ice. First, the equations describing both the vertical and horizontal plate viscous deformations have been derived, and were then solved by applying the finite element method. The accuracy of the discrete method has been verified by comparing the results predicted for a one-dimensional creep buckling problem

with the analytical results. The solution of the latter problem shows that the maximum plate deflections, occurring just before the critical time at which the plate begins to fail is reached, are, for the ice viscosities adopted, of the order of the ice thickness. Next, the numerical simulations for a two-dimensional problem of a large ice field driven by wind drag forces past an engineering structure in the form of a rectangle in the horizontal plane have been carried out. The results of calculations have shown that, at least for the particular structure geometries considered, the magnitudes of total horizontal forces exerted by ice on the structure, do not change considerably with wind direction. The effect of ice thickness, temperature and type of anisotropy on the contact forces is also limited. On the other hand, the latter factors very significantly influence the critical times, at which the floating ice cover starts to break due to its flexural failure.

Acknowledgement

This work has been supported by the Polish Committee for Scientific Research (KBN) through grant No. 8 T07E 007 20.

References

Flato G. M. and Hibler W. D. (1992), Modelling Pack Ice as a Cavitating Fluid, *J. Phys. Oceanogr.*, **22** (6), 626–651.

Hibler W. D. (1979), A Dynamic Thermodynamic Sea Ice Model, *J. Phys. Oceanogr.*, **9**, 815–845.

Morland L. W. and Staroszczyk R. (1998), A Material Coordinate Treatment of the Sea-ice Dynamics Equations, *Proc. R. Soc. Lond.*, A **454** (1979), 2819–2857.

Overland J. E. and Pease C. H. (1988), Modeling Ice Dynamics of Coastal Seas, *J. Geophys. Res.*, **93** (C12), 15619–15637.

Rothrock D. A. (1975), The Energetics of the Plastic Deformation of Pack Ice Ridging, *J. Geophys. Res.*, **80**, 4514–4519.

Sanderson T. J. O. (1988) *Ice Mechanics. Risks to Offshore Structures*, Graham and Trotman, London.

Schulkes R. M. S. M., Morland L. W. and Staroszczyk R. (1998), A Finite-element Treatment of Sea Ice Dynamics for Different Ice Rheologies, *Int. J. Numer. Anal. Meth. Geomech.*, **22** (3), 153–174.

Smith G. D. and Morland L. W. (1981), Viscous Relations for the Steady Creep of Polycrystalline Ice, *Cold Reg. Sci. Technol.*, **5** (2), 141–150.

Smith R. B. (1983), A Note on the Constitutive Law for Sea Ice, *J. Glaciol.*, **29** (101), 191–195.

Staroszczyk R. and Hedzielski B. (2003), Creep Buckling of a Wedge-shaped Floating Ice Plate, *Eng. Trans.*, In press.

Timoshenko S. and Woinowsky-Krieger S. (1959), *Theory of Plates and Shells*, McGraw-Hill, New York, 2nd ed.

Zienkiewicz O. C. and Taylor R. L. (1991), *The Finite Element Method*, Vol. 2. McGraw-Hill, London, 4th ed.